INTERNATIONAL
Agrophysics
www.international-agrophysics.org

Int. Agrophys., 2025, 39, 41-51
doi: 10.31545/intagr/195154

Mechanical characterization of failure mechanisms during the cutting of *Caragana korshinskii* Kom. branches**

Qiang Su, Zhihong Yu, Wenhang Liu, Xuejie Ma, Jianchao Zhang, Zhixing Liu*

College of Mechanical and Electrical Engineering, Inner Mongolia Agricultural University, Hohhot 010018, China

Received June 5, 2024; accepted October 23, 2024

A b s t r a c t. The mechanical properties related to the failure of *Caragana korshinskii* Kom. branch is critically important for the design of stem crushers. This paper studies *Caragana korshinskii* Kom. branch, focusing on shear and transverse compression tests. When the external load surpasses the strength limit, the internal structure of *Caragana korshinskii* Kom. branch undergoes damage and cracking. As cracks accumulate, expand, and fuse, CKB deforms and fractures. The failure process is characterized by elastic, elastoplastic, and plastic fracture, indicating that the yield strength varies. The sampling position and moisture content significantly influence the maximum shear strength and compressive strength, with the sampling position being particularly impactful. Shear and transverse compression tests illustrate the development process of CKB. Additionally, second-order response models for the relationship of the CKB moisture content, sampling location, and loading rate with shear strength and compressive strength were constructed. The p-values of the models were all less than 0.01, with determination coefficients exceeding 0.98, adjusted determination coefficients over 0.96, and coefficients of variation being 8.78 and 6.51%, respectively. Furthermore, the shear failure range spanned from 37.25 to 158.94 MPa, and the compression failure range extended from 12.32 to 63.93 MPa. In summary, to achieve effective chopping of CKB, the applied force must exceed the maximum shear strength of 158.94 MPa and the compressive strength of 63.93 MPa.

K e y w o r d s: *Caragana korshinskii* Kom. branch, crushing, mechanical properties, response surface testing, sampling position

*Corresponding author e-mail: yzhyqyzhyq@126.com

**National Natural Science Foundation of China (52265035), Inner Mongolia Autonomous Region Natural Science Foundation (2022MS05049), Research Program of science and technology at Universities of Inner Mongolia Autonomous Region (NJZZ23047), Program for improving the Scientific Research Ability of Youth Teachers of Inner Mongolia Agricultural University (BR230154).

1. INTRODUCTION

Caragana korshinskii Kom. branch (CKB) is a primary shrub for vegetation restoration in arid areas and is also an ideal biomass energy crop with the characteristics of high calorific value and strong germination ability (Wang *et al*., 2020; Long *et al*., 2020; Zhao *et al*., 2021). To ensure the vigorous growth of CKB, pruning is required every 3-5 years (Xu *et al*., 2020; Gao *et al*., 2021). This will result in accumulating a substantial amount of CKB, increasing the risk of forest fires. In Inner Mongolia, the stubble area of *Caragana korshinskii* Kom. in 2023 was 9.6×10^8 m^2, with a CKB harvest volume of 4.5 kg m^{-2} (wet). The market price of CKB powder (crushed CKB) is 1.2 yuan (kg)$^{-1}$, and the total output value can reach 52 billion yuan. Effective crushing can expedite the resource utilization of CKBs, thereby enhancing economic benefits. Understanding the mechanical properties of CKB is crucial for selecting appropriate crushing methods, studying crushing mechanisms, and developing effective crushing equipment for post-harvest processing.

Crushing is an essential link in the resource utilization of agricultural waste and serves as a robust guarantee for enhancing the quality and economic benefits of waste-derived products (Gunaratne *et al*., 2020; Möllnitz *et al*., 2020; Khodier *et al*., 2021). Mechanized crushing represents an inevitable trend and an essential step for the

high value-added recycling of CKB; however, it currently faces such issues as low crushing efficiency and high energy consumption. Research indicates that the physical and mechanical properties of crop stems form the foundation for the development of agricultural machinery (Aydın and Arslan, 2018; Wang *et al*., 2020). Ray and Bret-Harte (2019) conducted experiments on the viscoelastic bending behaviour of shrubs, furthering the understanding of plant stem mechanics. Zhao *et al*. (2024) employed a state-of-the-art microcomputer-controlled universal testing machine to examine the tensile, compression, bending, and shear properties of poplar branches, offering crucial data for improving the design of pruning and crushing machinery. Zhang *et al*. (2024) investigated the static mechanical properties of *Salix salix* and *Caragana korshinskii* Kom. They measured twelve elastic constants for both species using electrical methods and confirmed that these constants align with the orthotropic model. Li *et al*. (2024) examined *Caragana korshinskii* Kom. to analyze its mechanical properties in both transverse and along-grain directions under dynamic impact loads. They developed a stress-strain curve to define the cutting behaviour of *Caragana korshinskii* Kom., establishing a foundational model. Numerous factors influence the mechanical properties of stems. Wang *et al.* (2021) studied the tensile, shear, and bending mechanical properties of *Salix psammophila* branches during winter dormancy, analyzing the impacts of branch length, diameter, and chemical composition on these properties, and identified shear force as the type of external force most likely to damage the branches. Qiu *et al*. (2019) measured the mechanical properties of CKB in various parts and growth stages, including tensile strength, shear strength, and elastic modulus. These studies provided a quantitative analysis of the mechanical properties of CKB but did not explore the failure process under stress or the impact of moisture content. Furthermore, as a critical factor, moisture content significantly influences the mechanical properties of crop stems, garnering considerable attention from scholars (Okyere *et al*., 2022). Christensen-Dalsgaard and Ennos (2012) experimentally demonstrated that woody plants subjected to drought conditions exhibit, on average, stiffer and stronger stems compared to those grown in normal water supply conditions. Kumar *et al*. (2023) analyzed the bending stress, elastic modulus, and cutting energy of cotton stalks. Boydaş *et al*. (2019) investigated the effects of moisture content, internode area, and bevel angle on shear stress, specific shear energy, bending stress, and elastic modulus of hop stems during bending. Both shear stress and specific shear energy decreased as moisture content decreased. Both bending stress and elastic modulus decreased with increasing moisture content. The cutting strength of hop stems significantly decreased with increasing moisture content. Moisture content had a highly significant impact on the cutting strength of Marco Polo. The optimal cutting parameters for hop stems were identified as fresh samples, a 100 mm min^{-1} cutting speed, and a sliding cutting mode (Yang *et al*., 2022). In summary, domestic and international scholars have extensively researched the physical and mechanical properties of plant stems, thereby informing the design and process analysis of agricultural machinery and equipment (Chen *et al*., 2023). However, the structure of CKB is complex, and their texture is relatively hard, necessitating further research to enrich the understanding of the mechanical properties of failed stems.

This study investigates the mechanical properties associated with the cutting failure of CKB. Shear and transverse compression tests were conducted using CKB as the research subject. The response surface methodology was applied to analyze the impact of moisture content, sampling location, and loading speed on the shear and transverse compression properties of CKB. A second-order response model was developed to describe the relationship between individual factors (moisture content, sampling location, loading rate) and their interactions on the shear and transverse mechanical properties. This study analyzes the effects of both individual factors and their interactions on the shear and transverse compression properties, offering theoretical insights for the optimization of the CKB chopping technology.

2. MATERIAL AND METHODS

Figure 1 illustrates the chopping effect on CKB, revealing an uneven material texture and poor chopping performance. Investigating the mechanical properties of CKB is crucial for enhancing crushing efficiency. Research indicates that, during chopping, CKB are predominantly influenced by shear force and lateral extrusion force (Liang *et al*., 2020). Consequently, this study focused solely on evaluating the shear and transverse compression mechanical properties of CKB.

In August 2023, CKB samples were collected from Helinger County, Inner Mongolia, China (40º9′36″E, 111°48′N). Straight-stemmed plants with healthy growth, minimal branching, few signs of disease or pests, and no

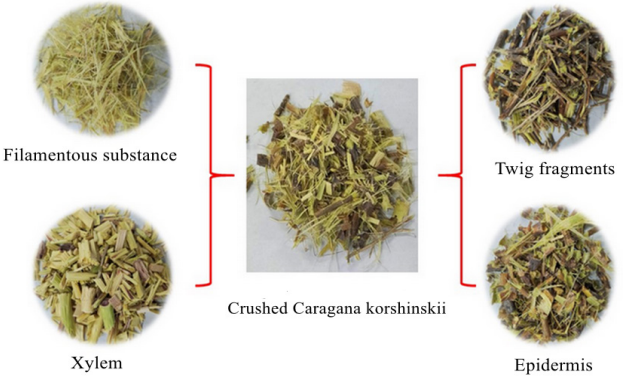

Fig. 1. Distribution of CKB post-crushing.

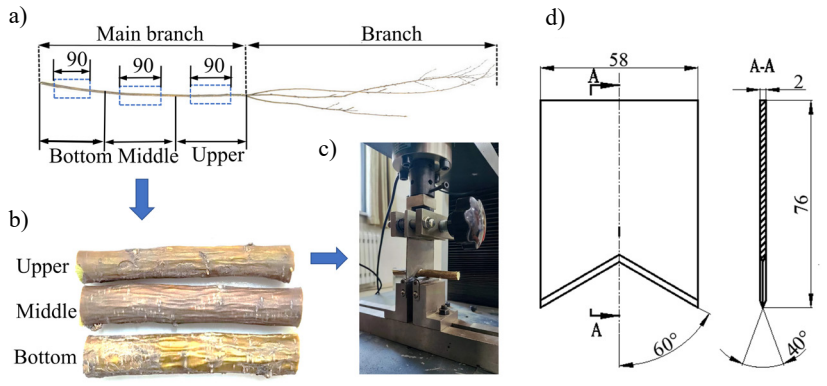

Fig. 2. Sample and scheme of the CKB test: a) sampling location, b) shear test samples, c) shear test d) cutting tool 2D diagram.

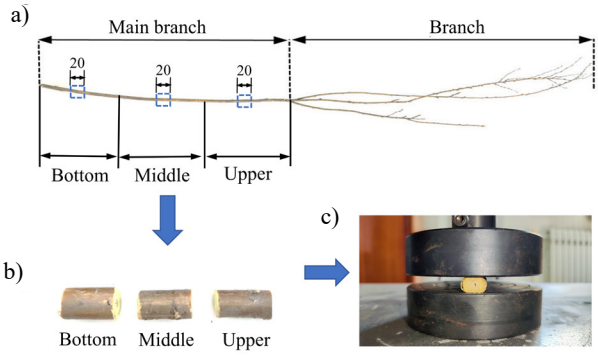

Fig. 3. Sample and scheme of the CKB test: a) sampling location, b) compression test sample, c) compression test.

visible damage were randomly selected. The CKB strips were cut 5-10 cm above the ground surface, wrapped with cling film to prevent water loss, and transported to the laboratory. Statistical analysis of the basic parameters of CKB showed that the maximum value of CKB height was 1.8 m, and the minimum value was 0.9 m. The average height of CKB was 1.2 m, and the diameter ranged from 5.34 to 12.21 mm. Cutting off the lateral branches and leaf buds and measuring the moisture content at the bottom cut of the CKB strips with the DHG-9140A electric thermostatic blast drying oven (temperature control accuracy: 0.1°C), the moisture content of the fresh CKB was 42.21±1.5%. The density of the CKBs was 984.70 kg m^{-3}, measured by the overflow as a volumetric method.

The main branches of the CKB material were divided into upper, middle, and bottom, from which specimens were prepared. Figure 2 presents the shear test specimen and corresponding test equipment. The shear test specimen had a length of 90±0.5 mm (Fig. 2a, b). The shear blade was made of 75Cr1, a material known for its high hardness, with dimensions detailed in Fig. 2c, d. Figure 3a, c illustrates the compression test specimen and the instrument. The compression test specimen had a length of 20 ± 0.5 mm. Stem nodes were carefully avoided during the sample preparation process. The diameters of the test samples were statistically analyzed, as presented in Table 1.

Due to the high moisture content of harvested CKB, which can clog crushing machinery, drying is required. To investigate how moisture content affects the failure mechanics of CKB, this study varied the moisture content. The method for modulating the moisture content is as follows: Place the sample in an electric blast drying oven and dry it for 8 h at 103±2°C. Select and weigh several samples every 2 h, comparing their masses. If the relative change is

Table 1. Statistics of sample diameters

Types	Shear sample			Compression sample		
Sampling location	Upper	Middle	Bottom	Upper	Middle	Bottom
Maximum values	8.51	10.12	11.28	9.47	9.93	11.90
Minimum value	7.03	7.78	9.64	7.92	8.59	10.02
Average value	7.73	8.27	10.29	8.48	9.29	10.57
Standard deviation	0.44	0.49	0.50	0.46	0.31	0.50
Variation coefficient (%)	5.72	5.42	4.82	5.43	3.33	4.78

Table 2. Technical parameters of the SDJF-20KN universal testing machine

Parameter	Value/unit
Test distance accuracy	0.1 N
Test force accuracy	±0.5%
Sensors	Built-in pressure sensor
Test speed range	0.005~500 mm min^{-1}
Power range	0~20 kN
Test distance range	0~600 mm
Operating temperature	10~35°C

within 0.5%, the sample is deemed completely dry. Soak the dried sample in clean water for 72 h, and then store it in a refrigerator at 4°C until the water is evenly absorbed. Adjust the test moisture content according to the desired gradient using an electric blast drying oven set at 60±2°C.

Following the completion of moisture content modulation, referring to GB/T 1935-2009 and GB/T 1937-2009 standards for wood and timber and test procedures, CKB were tested in shear and compression tests using the SDJF-20KN universal testing machine (SDJF-20KN, Zhuodi Instrument and Equipment (Beijing) Co., Ltd). Table 2 shows the technical parameters of the equipment. The test machine mainly consists of a support indenter, transducer, and control system, as shown in Fig. 3a. For the test, the specimen is placed on the support, and the upper indenter is adjusted so that when the upper indenter is in contact with the specimen, it moves downward at the speed required for the test. Then, the upper indenter was adjusted to move downward at the speed required for the test when the upper indenter was in contact with the specimen. The computer records the pressure-deformation curve in real time. When the curve's pressure value (longitudinal coordinate) shows a sudden change, the specimen has cracked, and the loading stops. Higher loading rates can increase the material's strength and stiffness, whereas lower rates may better reflect the real-world conditions or the stalk's long-term performance (Muzamil *et al*., 2016). Additionally, to account for the loading rate and ensure operational safety of the universal testing machine, the loading speeds were set at 10, 20, and 30 mm min^{-1}, respectively.

To investigate the factors influencing the mechanical properties of CKB failure, the moisture content (A), sampling position (B), and loading rate (C) were selected as experimental variables. Using shear strength (τ_j) and critical compressive strength (σ_y) as response variables, the shear and compressive strengths can be determined based on CKB and mechanical testing dimensions (Yi *et al*., 2020):

$$\tau_j = \frac{2F^j_{max}}{\pi d^2}, \quad (1)$$

where: τ_j is the shear strength (MPa), F^j_{max} is maximum shear load (N), d is sample diameter (mm).

Table 3. Experimental factors and levels

Level	Experimental factors		
	A Moisture content (%)	*B* Sampling location	*C* Loading rate (mm min^{-1})
-1	10±2	Upper	10
0	30±2	Middle	20
1	50±2	Bottom	30

Calculation formula for compressive strength of CKB (Al-musawi *et al*., 2023):

$$\sigma_y = \frac{4F^y_{max}}{\pi d^2}, \quad (2)$$

where: σ_y is compressive strength (MPa), F^y_{max} is the maximum compressive load (N), d is the specimen diameter (mm).

To determine the influence of various factors on the mechanical properties of CKB failure, the moisture content (A) of the stems was adjusted to 10, 30, and 50% using the previously described method. Sampling positions were categorized into upper, middle, and bottom, and the loading rate (C) gradient was set at 10, 20, and 30 mm min^{-1} (Radmanović *et al*., 2021). These speed ranges align with the guidelines set forth in GB/T 1935-2009 and GB/T 1937-2009 (Standards GB/T 1935-2009, 2009; Standards GB/T 1937-2009, 2009; Liang *et al.*, 2020), which address the determination of shear and static compressive strength of wood. This framework elucidates the mechanical behaviour of CKB under a lower loading rate. The response surface methodology was employed to conduct an orthogonal experimental design using Design-Expert 11 software. This involved seventeen test groups, each with five replications. The experimental factors and their levels are presented in Table 3.

3. RESULTS AND DISCUSSION

The crushing mode of CKB depends on their mechanical properties. The test of failure mechanical properties of CKB is shown in Fig. 4. Figure 4a depicts the electronic universal testing machine. Figure 4b illustrates the fracture failure of the shear test specimen, showing a distinct gradual fracture of cellulose. Figure 4c depicts the failure of CKB under transverse compression, revealing the crack extension phenomenon. This observation is comparable to the compression process observed in cotton stalks (Zhao *et al*., 2023).

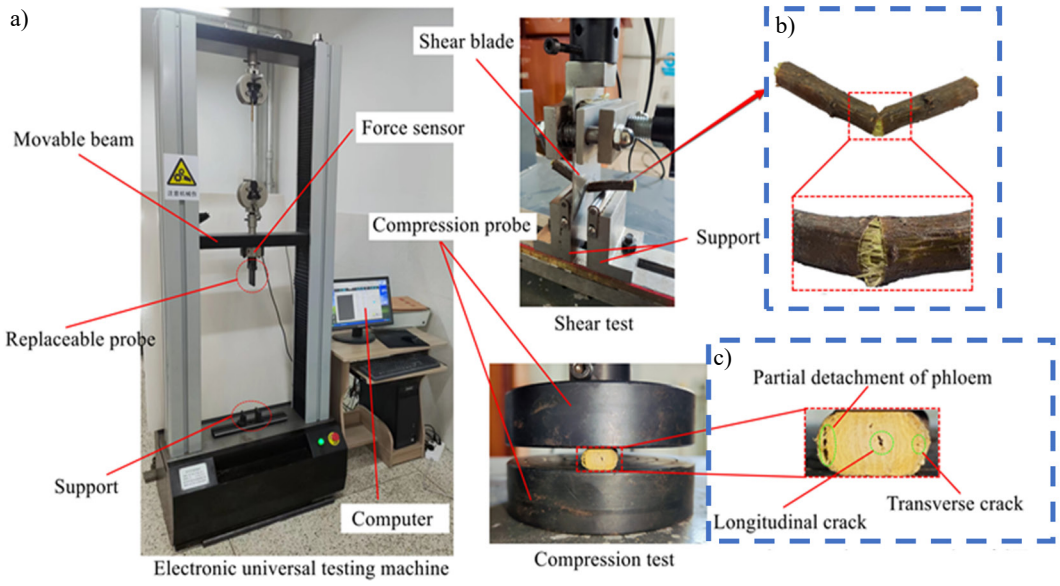

Fig. 4. Mechanical tests and instruments for CKB: a) test equipment, b) shear failure, c) compression failure.

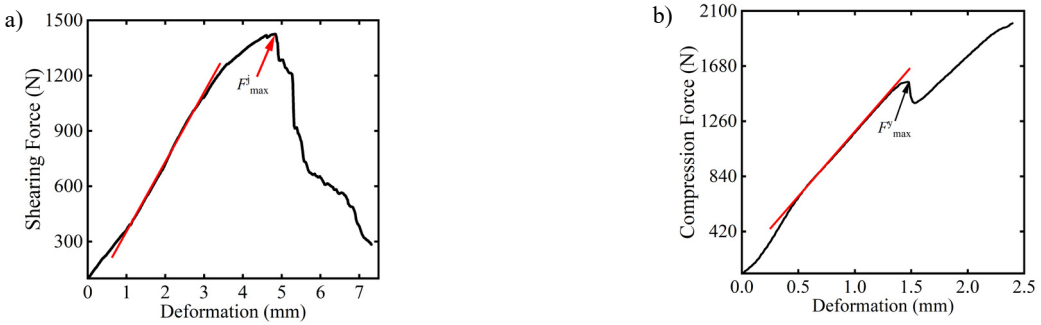

Fig. 5. Shear load displacement curve of CKB: a) shear force, b) compression force.

A sample of shear and compression test data was selected to analyze the trends in the force-displacement changes. Figure 5a presents the force-displacement curves from the shear test. Initially, the curve shows nonlinear growth, with the shear force increasing as the displacement rises. As the displacement continues, the shear force transitions to linear elasticity. During the yield stage, the deformation accelerates while the load increases more slowly until reaching its peak, indicating CKB failure. Post-fracture, the deformation increases and the shear load fluctuates due to vascular bundles in the xylem approaching their fracture limit and a gradual reduction in shear strength. The load-deflection diagrams of CKBs indicate they behave similarly to elastic-plastic materials, exhibiting both elastic deformation and yield fracture stages.

Figure 5b shows that the maximum compressive load of CKB reached more than 2000 N, significantly different from the value of the maximum compressive load of cannabis stalks studied by Khan *et al*. (2010). The complex woody structure of CKBs significantly increases the resistance to external forces compared to the hollow cannabis stalks. The compression process can be divided into four stages. The initial loading stage is where the deformation is less sensitive to force. The reason may be that the phloem is dewatered and deformed and closely associated with the xylem, and smaller forces are not enough to cause damage to the CKB. As the compression test proceeded, the load increased linearly with the deformation, indicating that the CKB strips were gradually densified under the force and showed compressive properties. As the deformation continued to increase, the compression force tended to increase and then decrease, possibly due to the increase in the compression load, which reached the maximum bearing capacity of the CKB. The CKB crushed, leaving the remaining vascular bundles to bear the force exerted on the specimen, so the compression load decreased sharply. The specimen then regained its compressive capacity, and with the gradual increase in the compressive load, the CKBs entered the compression strengthening stage, and the test was terminated.

During each shear and compression process, the damage and cracking of the internal structure of CKB occurs when the external load exceeds the strength limit. CKB undergoes deformation and cracking, developing from elastic to plastic deformation with the accumulation, expansion, and fusion of the cracks. The difference between the two is that, under shear, the cracks gradually expand and finally fracture, producing irrecoverable plastic deformation. In the compression process, after reaching the maximum compressive strength, with the increase in the external load, the internal organization of CKB is gradually densified, and the compressive strength gradually increases. From the perspective of shear and compression forces on CKB, the values of stem damage are not uniform. This variability arises because the mechanical properties of the stems are influenced by such factors as moisture content, plant maturity, internode position, soil type, and temperature (Leblicq *et al*., 2015).

Table 4 shows the shear and compression test results for CKB specimens with different the moisture content (A) and sampling position (B) under different loading rates (C).

Table 5 shows the ANOVA results of the response surface test. The analysis of variance (ANOVA) module in Design Expert 11 software was utilized. The second-order response models of shear and compressive strengths for different moisture contents (A), different sampling positions (B), and different loading rates (C) were developed, and the degree of the influence of the single-factor term and its interaction term on the mechanical properties of CKB was analyzed.

Based on the regression ANOVA analysis of the results of the CKB shear test shown in Table 5, it can be seen that the single factor terms A ($p=0.0009<0.01$) and B ($p<0.0001$) and the interaction term B^2 ($p<0.0001$) were highly significant factors affecting the shear strength. The interaction term AB ($p=0.0204\leq0.05$) significantly affected the shear strength. The other single factor terms and interaction terms with $p>0.05$ were non-significant factors for τ_j. Therefore, the order of significant influences affecting shear strength is $B>A>B^2>AB$. Based on regression ANOVA, the second-order response model of shear strength τ_j versus the moisture content (A), sampling position (B), and loading rate (C) was constructed as:

$$\tau_j=59.35-17.63A+35.83B+0.0907C-9.62AB-1.82AC -0.1511BC+6.65A^2+34.99B^2-9.63C^2. \quad (3)$$

The p-value coefficient of the model shear strength τ_j is much less than 0.0001, with the coefficient of determination $R^2=0.9849$, the corrected coefficient of determination $R^2_{adj}=0.9656$, the coefficient of variation $C.V.=8.78\%$, and the predicted coefficient of determination $R^2_{Pred}=0.8451$. The factors influencing the moisture content (A), sampling position (B), and loading rate (C) are highly correlated with the shear strength τ_j. They have a high correlation. If the non-significant factors affecting the shear strength are neglected, the second-order response model can be simplified as follows:

$$\tau_j=59.35-17.63A+35.83B-9.62AB+34.99B^2. \quad (4)$$

Table 4. Experimental design and results

Run	A	B	C	τ_j (MPa)	σ_y (MPa)
1	-1	1	0	158.45±10.23	63.91±3.56
2	0	0	0	50.64±1.39	27.06±3.32
3	1	0	1	47.47±3.45	24.82±1.32
4	1	-1	0	56.74±2.48	12.32±2.29
5	0	-1	-1	42.98±4.39	17.19±4.01
6	0	-1	1	33.04±5.68	16.75±3.27
7	-1	0	1	72.85±7.34	42.14±2.63
8	0	1	1	123.12±4.19	56.22±6.85
9	30	0	0	60.61±2.15	32.39±4.70
10	0	0	0	58.30±4.74	32.24±2.31
11	-1	0	-1	65.61±6.54	39.05±4.22
12	1	0	-1	47.51±7.76	33.67±5.81
13	0	1	-1	126.67±3.98	58.89±5.04
14	0	0	0	64.16±5.34	33.91±6.92
15	0	0	0	63.02±2.98	32.24±5.26
16	-1	-1	0	66.28±7.35	20.63±3.85
17	1	1	0	110.43±10.61	55.07±7.23

Based on the regression ANOVA analysis of the results of the CKB compression test shown in Table 5, it can be seen that the single factor terms A ($p=0.0002\leq0.01$) and B ($p<0.0001$) and the interaction term B^2 ($p<0.0001$) were the highly significant factors affecting the compressive strength. The interaction term AC ($p=0.0242\leq0.05$) significantly affected the compressive strength. All other single-factor and interaction terms had p-values >0.05 and were insignificant in affecting compressive strength. Therefore, the significant shear strength influences are $B>A>B^2>AC$. Based on the regression ANOVA, the second-order response model of compressive strength σ_y versus the moisture content (A), sampling position (B), and loading rate (C) was constructed as:

$$\sigma_y=31.57-4.98A+20.9B-1.11AB-0.1355AB-2.98AC -0.5563BC+2.04A^2+4.38B^2+1.31C^2. \quad (5)$$

The p-value of the model compressive strength (σ_y) is much less than 0.0001, with a coefficient of determination $R^2=0.9910$, a corrected coefficient of determination $R^2_{adj}=0.9795$, a coefficient of variation $C.V.=6.51\%$, and a predicted coefficient of determination $R^2_{Pred}=0.9564$. This suggests that the factors influencing the moisture content (A), sampling position (B), and loading rate (C) are highly

Table 5. Regression variance analysis of the mechanical characteristic test results of cotton stalks

Source	df	τ_j (MPa)				σ_y (MPa)			
		Sum of squares	Mean squares	F value	p-value	Sum of squares	Mean squares	F value	p-value
Model	9	19013.09	2112.57	50.86	<0.0001**	3920.66	435.63	86	<0.0001**
A	1	1276.25	1276.25	30.72	0.0009**	323.19	323.19	63.8	<0.0001**
B	1	1.28×10^5	1.28×10^5	307.43	<0.0001**	3452.27	3452.27	681.53	<0.0001**
C	1	4.92	4.92	0.1185	0.7408	9.84	9.84	1.94	0.2061
AB	1	370.18	370.18	8.91	0.0204*	0.5944	0.5944	0.1174	0.742
AC	1	13.23	13.23	0.3185	0.5901	35.6	35.6	7.03	0.0329*
BC	1	10.23	10.23	0.2462	0.635	1.24	1.24	0.2444	0.6362
A^2	1	254.26	254.26	6.12	0.0426*	1.84	1.84	0.3628	0.566
B^2	1	4010.05	4010.05	96.54	<0.0001**	85.31	85.31	16.84	0.0046**
C^2	1	322.78	322.78	7.77	0.027*	5.95	5.95	1.17	0.3143
Residual	7	290.77	41.54			35.46	5.07		
Lack of Fit	3	175.59	58.53	2.03	0.2519	8.11	2.7	0.3951	0.7642
Pure Error	4	115.19	28.8			27.35	6.84		
Cor Total	16	19303.86				3956.12			
		$R^2=0.9849$, Adjusted $R^2=0.9656$				$R^2=0.9910$, Adjusted $R^2=0.9795$			
		C.V.=8.78%, Predicted $R^2=0.8451$				*C.V.*=6.51%, Predicted $R^2=0.9564$			

*Significant factor ($0.01<p\leq0.05$), **extremely significant factor ($p\leq0.01$), $p>0.05$ non-significant factor.

correlated with compressive strength (σ_y). If the non-significant factors affecting the compressive strength are neglected, the second-order response model can be simplified as follows:

$$\tau_j = 31.57 - 4.98A + 20.9B - 2.98AC + 4.38B^2. \quad (6)$$

In summary, the water content (A) and sampling location (B) significantly influence both the shear strength and the compressive strength. In contrast, the loading speed (C) has a relatively minor effect on these properties.

In order to better observe the trend of the influence of different test factors on the shear strength and compressive strength, two of the three factors mentioned above were fixed at the center level 0 point to obtain the influence pattern of another influence factor on the shear strength and compressive strength. As shown in Fig. 6a, the shear strength of CKB decreases significantly when its moisture content (A) is between 10 and 30%. However, when the moisture content (A) increases from 30 to 50%, the shear strength of CKB rises.

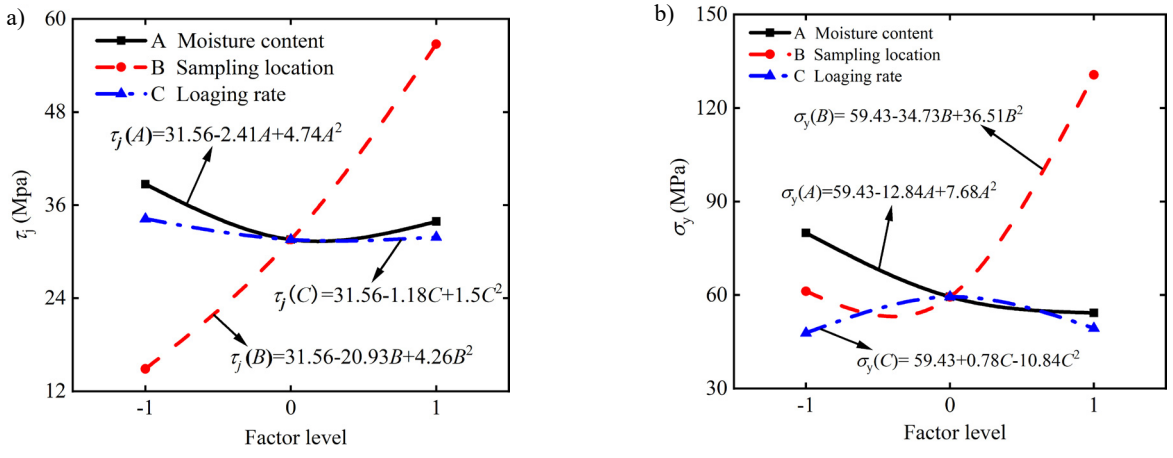

Fig. 6. Effect of individual factors on the shear strength and compressive strength of CKB: a) shear strength (τ_j), b) compressive strength (σ_y).

As shown in Fig. 6b, the trend of the effect of moisture content (A) on compressive strength is quite different from the effect of moisture content (A) on shear strength. With the increasing moisture content (A), the compressive strength showed a linear decrease trend. The reason may be that when the moisture content (A) is low, the CKB specimens have greater stiffness and higher load-bearing capacity; when the moisture content (A) increases, the CKB forms a higher expansion pressure to resist the deformation (Li *et al*., 2022), resulting in a decrease in the load-bearing capacity, which is more pronounced in the case of 50% moisture content (A). The CKB damage pattern will also be changed when the moisture content is too high. Therefore, the relationship between the moisture content (A) and the shear strength (τ_j) and compressive strength (σ_y) of CKB was modeled as follows:

$$\begin{cases} \sigma_y(A)=59.43-12.84A+7.68A^2 \\ \tau_j(A)=31.56-2.41A+4.74A^2 . \end{cases} \quad (7)$$

As shown in Fig. 6a and 6b, the effect of the sampling position (B) on the shear and compressive strength of CKB is significant. When the sampling position (B) is in the upper part of the CKB (level 1), the corresponding shear strength and compressive strength are at the lowest. When the sampling position (B) is in the lower part of the CKB (level -1), the corresponding shear and compressive strengths are the highest. The significant difference between the two sampling positions is closely related to the CKB's growth structure and flat stubble characteristics. At regular intervals, CKBs must be stubbled to ensure they thrive, and most of the stubbled areas are the roots. Consequently, the CKB's bottom, which has a prolonged growth period and a dense xylem, exhibits high hardness. The shear and compressive strengths of the bottom are notably greater than those of the upper portions. In this case, the relationship model between sampling position B and shear strength and compressive strength is as follows:

$$\begin{cases} \sigma_y(B)=59.43-34.73B+36.51B^2 \\ \tau_j(B)=31.56+20.93B+4.26B^2 . \end{cases} \quad (7)$$

The maximum shear force of CKBs gradually decreased as the sampling position of CKBs changed gradually from the lower to the upper part. This study is in line with the findings of Zhao *et al*. (2022) and others on the mechanical properties of mature broccoli during growth, who concluded that the closer the mature broccoli is to the top, the lower the proportion of fibrous tissue and xylem is, which leads to a gradual decrease in the shear force of the mature broccoli. Igathinathane conducted a shear test on maize stalks, and the results also showed that the bottom of the stalk had more excellent resistance to external loading than the middle and top of the stalk (Igathinathane *et al*., 2010). In addition, such factors as the diameter of the selected specimen and the cellulose content should be considered as influencing factors for the variation of mechanical properties (Ma *et al*., 2019).

As shown in Fig. 6, the differences in shear and compressive strength were evident as the loading rate (C) increased. When the loading rate (C) increased from 10 to 20 mm min^{-1}, the shear strength of CKB increased significantly; when the loading rate (C) further increased from 20 to 30 mm min^{-1}, the shear strength of CKB gradually decreased. When the loading rate (C) increased from 10 to 20 mm min^{-1}, the compressive strength of the CKB decreased significantly; when the loading rate (C) was further increased from 20 to 30 mm min^{-1}, the compressive strength of the CKB remained unchanged. Also, the loading rate (C) has little effect on CKB's shear and compressive mechanical properties. The relationship between the loading rate (C) and shear strength and compressive strength is modeled as follows:

$$\begin{cases} \sigma_y(C)=59.43+0.78C-10.84C^2 \\ \tau_j(C)=31.56-1.18C+4.26C^2 . \end{cases} \quad (9)$$

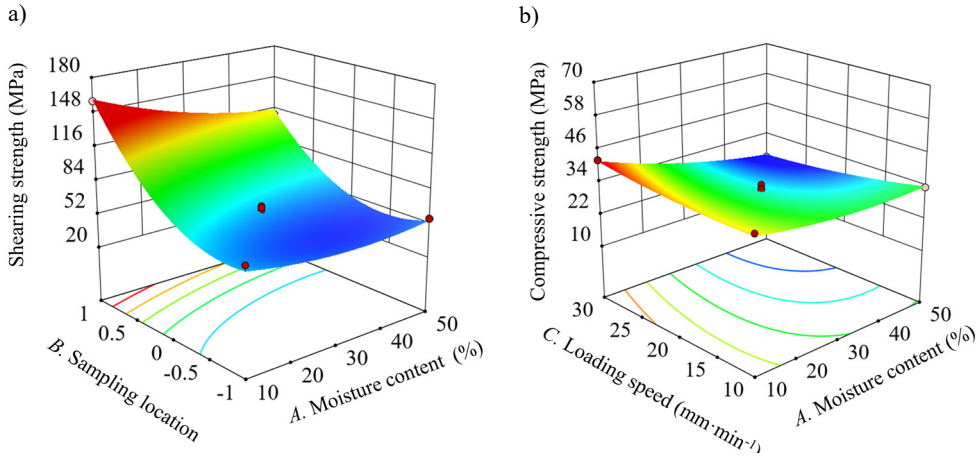

Fig. 7. Response surface the influence trend of interaction: a) term AB on shear strength, b) term AC on compressive strength.

The results of regression ANOVA in Table 5 show that the interaction term *AB* significantly influences the shear strength, *i.e.*, the interaction between the moisture content (*A*) and the sampling location (*B*) significantly affects the shear strength. Therefore, this part of the analysis ignored other insignificant interaction terms and only analyzed the change rule of the effect of the interaction term *AC* on τ_j.

Figure 7a illustrates how shear strength interacts with the moisture content (*A*) and the sampling location (*B*). When the moisture content (*A*) of CKB ranges from 10 to 30%, its shear strength decreases steadily with increasing moisture. In contrast, when the moisture content (*A*) rises from 30 to 50%, the rate of the increase in the shear strength is less pronounced, compared to the 10-30% range. Additionally, as the sampling location (*B*) moves from the top to the root, the shear strength consistently increases.

Figure 7b shows the trend of the effect of the interaction of the moisture content *(A)* and the loading rate (*C*) on the compressive strength of CKB. The compressive strength of CKB varied significantly with the change in the moisture content (*A*). When the level was -1~1, *i.e*., when the moisture content (*A*) of CKB strips was varied from 10 to 50%, the compressive strength of CKB tended to decrease, the same as the results of the one-way analysis. When the loading rate (*C*) was varied within the horizontal range of -1~1, *i.e*., when the loading rate (*C*) was 10~30 mm min^{-1}, the compressive strength of CKB tended to decrease gradually with the increase in the loading rate (*C*), which was the same as the results of one-factor analysis. The compressive strength of CKB still had a significant tendency to decrease as both levels varied from low to high due to the effect of both interactions.

Currently, the primary methods for straw crushing are knife cutting and hammer striking. To achieve effective cutting or crushing of CKBs, the applied external load must exceed the shear strength and compressive strength of the stalks. With a moisture content (*A*) of 10.12%, a sampling position at the lower part (*B*), and a loading rate (*C*) of 25.27 mm min^{-1}, the theoretical maximum shear and compressive strengths are 158.94 and 63.93 MPa, respectively. Conversely, suppose the sampling position is at the upper part. In that case, the theoretical minimum shear and compressive strengths are 37.25 and 12.32 MPa, respectively, with a loading rate (*C*) of 30 mm min^{-1} and a moisture content (*A*) of 46.84%. In summary, to achieve effective chopping of CKB, the applied force must exceed the maximum shear strength of 158.94 MPa and the compressive strength of 63.93 MPa. This consideration is crucial for the tool's geometric design, material selection, and motion mode, as the tool must handle higher cutting resistance. Strategies to address this include enhancing the sharpness of the cutting edge, adjusting the cutting angle, and using materials with higher hardness (Su *et al*., 2024).

From the perspective of the test material, the test samples were standardized in shape and size, resulting in relatively uniform results. However, achieving consistency in actual samples can be challenging, potentially leading to significant result dispersion. From a kinetic standpoint, the cutting dynamics of CKB are complex. The shear and compression tests conducted with the universal testing machine at low speeds do not accurately reflect high-speed cutting conditions. The universal testing machine operates at a constant low speed, whereas actual mechanical equipment, such as high-speed rotary tools, operates faster. This speed discrepancy may result in differences in the cutting force and the cutting mode. High-speed cutting in real conditions can reduce the force per unit time significantly, a phenomenon not fully replicated by universal testing machines. Thus, while universal testing machine results are useful, they should be supplemented with actual equipment performance tests and simulations for more accurate tool design and optimization. The complexity of CKB material limits the shear and compressive strength ranges obtained in this study. Future research will incorporate additional test factors and a thorough examination of the microstructure to enhance the understanding of the mechanical properties of CKB.

4. CONCLUSIONS

This experiment focused on the stems of *Caragana korshinskii* Kom. branch cultivated in Inner Mongolia and utilized the response surface methodology to perform shear and transverse compression tests on these stems. The research conclusions are as follows:

1. Internal damage and cracks in the *Caragana korshinskii* Kom. branch lead to elastic deformation, evolving into a plastic fracture with non-unique yield strength. Both the sampling position and moisture content significantly influence the maximum shear and compressive strengths, with the sampling position being particularly critical. Shear and transverse compression tests demonstrate that the failure process of *Caragana korshinskii* Kom. branch involves the progression through the elastic, elastoplastic, and plastic fracture stages.

2. Second-order response models for shear and compressive strength were developed, considering the moisture content, sampling position, and loading rate of *Caragana korshinskii* Kom. branch. The p-values of these models were all below 0.01, the coefficients of determination exceeded 0.98, the adjusted coefficients of determination were above 0.96, and the coefficients of variation were 8.78 and 6.51%, respectively.

3. When the moisture content is 10.12%, with the sampling position at the bottom and a loading rate of 25.27 mm min^{-1}, the theoretical maximum shear and compressive strengths are 158.94 and 63.93 MPa, respectively. Conversely, when the sampling position is at the top of the *Caragana korshinskii* Kom. branch, with a loading rate of

30 mm min^{-1} and a moisture content of 46.84%, the theoretical minimum shear and compressive strengths are 37.25 and 12.32 MPa, respectively. Therefore, it is advisable to perform crushing within this parameter range. In summary, to achieve effective chopping of *Caragana korshinskii* Kom. branch, the applied force must exceed the maximum shear strength of 158.94 MPa and the compressive strength of 63.93 MPa.

Conflict of interest: The Authors declare that they have no conflict of interest.

Compliance with ethical requirements: This study does not contain any experiment involving human or animal subjects.

5. REFERENCES

Al-musawi, H., Huber, C., Grabner, M., Ungerer, B., Krenke, T., Matz, P., *et al*., 2023. Compressive strength of beech and birch at different moisture contents and temperatures. J. Materials Sci. 58(35), 13994-14008. https://doi.org/10.1007/s10853-023-08882-w

Aydın, İ., Arslan, S., 2018. Mechanical properties of cotton shoots for topping. Industrial Crops Products 112, 396-401. https://doi.org/10.1016/j.indcrop.2017.12.036

Boydaş, M.G., Çomakli, M., Sayinci, B., Kara, M., 2019. Effects of moisture content, internode region, and oblique angle on the mechanical properties of sainfoin stem. Turkish J. Agric. Forestry 43(2), 254-263. https://doi.org/10.3906/tar-1802-32

Chen, M., Xu, G., Wei, M., Li, X., Wei, Y., Diao, P., *et al.*, 2023. Optimization design and experiment on feeding and chopping device of silage maize harvester. Int. J. Agric. Biol. Eng. 16(3), 64-77. https://doi.org/10.25165/j.ijabe.20231603.7922

Christensen-Dalsgaard, K.K., Ennos, A.R., 2012. Effects of drought acclimation on the mechanical properties of Ochroma pyramidale, *Betula pendula* and *Acacia karroo* tree seedling stems. Forestry 85(2), 215-223. https://doi.org/10.1093/forestry/cpr061

Muzamil, M., Mani, I., Kumar, A., Lande, S., 2016. Influence of moisture content, loading rate and internode position on the mechanical properties of paddy and wheat straw. Int. J. Bio-Resource and Stress Management 7(2), 280-285. https://doi.org/10.23910/IJBSM/2016.7.2.1469b

Gao, Y., Kang, F., Kan, J., Wang, Y., Tong, S., 2021. Analysis and experiment of cutting mechanical parameters for *Caragana korshinskii* (C.k.) Branches. Forests 12(10), 1359. https://doi.org/10.3390/f12101359

Gunaratne, T., Krook, J., Andersson, H., Eklund, M., 2020. Potential valorisation of shredder fines: Towards integrated processes for material upgrading and resource recovery. Resources, Conservation Recycling 154, 104590. https://doi.org/10.1016/j.resconrec.2019.104590

Igathinathane, C., Womac, A.R., Sokhansanj, S., 2010. Corn stalk orientation effect on mechanical cutting. Biosys. Eng. 107(2), 97-106. https://doi.org/10.1016/j.biosystemseng.2010.07.005

Khan, Md. M.R., Chen, Y., Laguë, C., Landry, H., Peng, Q., Zhong, W., 2010. Compressive properties of Hemp (*Cannabis sativa* L.) stalks. Biosys. Eng. 106(3), 315-323. https://doi.org/10.1016/j.biosystemseng.2010.04.004

Khodier, K., Feyerer, C., Möllnitz, S., Curtis, A., Sarc, R., 2021. Efficient derivation of significant results from mechanical processing experiments with mixed solid waste: Coarse-shredding of commercial waste. Waste Manag. 121, 164-174. https://doi.org/10.1016/j.wasman.2020.12.015

Kumar, A., Nayak, A.K., Sharma, S., Senapati, A., Mitra, D., Mohanty, B., *et al*., 2023. Rice straw recycling: A sustainable approach for ensuring environmental quality and economic security. Pedosphere 33(1), 34-48. https://doi.org/10.1016/j.pedsph.2022.06.036

Leblicq, T., Vanmaercke, S., Ramon, H., Saeys, W., 2015. Mechanical analysis of the bending behaviour of plant stems. Biosys. Eng. 129, 87-99. https://doi.org/10.1016/j.biosystemseng.2014.09.016

Li, C., Zhang, H., Wang, Q., Chen, Z., 2022. Influencing factors of cutting force for apple tree branch pruning. Agriculture 12(2), 312. https://doi.org/10.3390/agriculture12020312

Li, C., Zhang, J., Cao, L., Zhang, X., 2024. Analysis of dynamic mechanical properties of Caragana korshinskii using split Hopkinson pressure bar test. J. Northeast Forestry Univ. 52(5), 102-106. https://doi.org/10.13759/j.cnki.dlxb.2024.05.004

Liang, R., Chen, X., Zhang, B., Peng, X., Meng, H., Jiang, P., *et al*., 2020. Tests and analyses on mechanical characteristics of dwarf-dense-early major cotton variety stalks. Int. Agrophys. 34(3), 333-342. https://doi.org/10.31545/intagr/122575

Long, Y., Liang, F., Zhang, J., Xue, M., Zhang, T., Pei, X., 2020. Identification of drought response genes by digital gene expression (DGE) analysis in *Caragana korshinskii* Kom. Gene 725, 144170. Q3. https://doi.org/10.1016/j.gene.2019.144170

Ma, Y., Wu, S., Zhuang, J., Tian, Y., Qi, H., Tong, J., 2019. The effect of lignin on the physicomechanical, tribological, and morphological performance indicators of corn stalk fiber-reinforced friction materials. Materials Res. Express 6(10), 105325. https://doi.org/10.1088/2053-1591/ab396b

Möllnitz, S., Khodier, K., Pomberger, R., Sarc, R., 2020. Grain size dependent distribution of different plastic types in coarse shredded mixed commercial and municipal waste. Waste Manag. 103, 388-398. https://doi.org/10.1016/j.wasman.2019.12.037

Okyere, F.G., Kim, H.T., Basak, J.K., Khan, F., Bhujel, A., Park, J., *et al*., 2022. Influence of operational properties and material's physical characteristics on mechanical cutting properties of corn stalks. J. Biosys. Eng. 47(2), 197-208. https://doi.org/10.1007/s42853-022-00140-2

Qiu, S., Cui, Q., Wu, Z., Li, X., Guo, Y., 2019. Shear strength of stalks of *Caragana korshinskii* at different ages. J. Shanxi Agric. Univ. (Natural Science Edition) 39(6), 107-112.

Radmanović, K., Roginić, R., Beljo Lučić, R., Jovanović, J., Jug, M., Sedlar, T., *et al*., 2021. Effect of a high loading rate on the compressive properties of beech wood in the longitudinal direction. BioResources 16(2), 4093-4105. https://doi.org/10.15376/biores.16.2.4093-4105

Ray, P.M., Bret-Harte, M.S., 2019. Elastic and irreversible bending of tree and shrub branches under cantilever loads. Frontiers Plant Sci. 10, 59. https://doi.org/10.3389/fpls.2019.00059

Su, Q., Liu, W., Ma, X., Zhang, J., Yu, Z., Liu, Z., *et al*., 2024. A nonlinear elastic-plastic model describing the bending and fracture behavior of *Caragana korshinskii* Kom. Branch wood. Wood Material Sci. Eng. 1-11. https://doi.org/10.1080/17480272.2024.2394106

Standard, C.I., 2009. GB/T 1935-2009. Method of testing in compressive strength parallel to grain of wood. Standardization Administration of the People's Republic of China. Beijing, CN.

Standard, C.I., 2009. GB/T 1935-2009. Method of testing in shearing strength parallel to grain of wood. Standardization Administration of the People's Republic of China. Beijing, CN.

Wang, T., Liu, H., Duan, C., Xu, R., Zhang, Z., She, D., *et al*., 2020. The eco-friendly biochar and valuable bio-oil from *Caragana korshinskii:* pyrolysis preparation, characterization, and adsorption applications. Materials 13(15), 3391. https://doi.org/10.3390/ma13153391

Wang, Z., Gerile Cui, T., Hao, X., Zhang, Y., Si, Q., 2021. Mechanical properties of the branches of *Salix psammophila* and its influencing factors. J. China Agric. Univ. 26(11), 84-96.

Wang, Y., Yang, Y., Zhao, H., Liu, B., Ma, J., He, Y., *et al*., 2020. Effects of cutting parameters on cutting of citrus fruit stems. Biosys. Eng. 193, 1-11. https://doi.org/10.1016/j.biosystemseng.2020.02.009

Xu, H., Wang, Z., Li, Y., He, J., Wu, X., 2020. Dynamic growth models for *Caragana korshinskii* shrub biomass in China. J. Environ. Manag. 269, 110675. https://doi.org/10.1016/j.jenvman.2020.110675

Yang, J., Ma, Z., Zhang, S., Li, X., Luo, H., Feng, Y., 2022. Experimental analysis on mechanical properties of different varieties hop stems. J. Physics: Conf. Series 2368(1), 012030. https://doi.org/10.1088/1742-6596/2368/1/012030

Yi, W., Yitan, Z., Yan, Y., Hongmei, Z., Changhui, Y., Yu, H., *et al*., 2020. Discrete element modelling of citrus fruit stalks and its verification. Biosys. Eng. 200, 400-414. doi.10.1016/j.biosystemseng.2020.10.020

Zhao, L., Zhou, H., Jin, S., Cui, W., Wang, M., 2024. Mechanical properties of poplar (NL-3412) branches. Wood Material Sci. Eng. 1-11. https://doi.org/10.1080/17480272.2024.2321278

Zhao, W., Chen, M., Xie, J., Cao, S., Wu, A., Wang, Z., 2023. Discrete element modeling and physical experiment research on the biomechanical properties of cotton stalk. Computers Electronics Agric. 204, 107502. https://doi.org/10.1016/j.compag.2022.107502

Zhao, Y., Tang, Z., Chen, S., 2022. Loading Model and Mechanical Properties of Mature Broccoli (*Brassica oleracea* L. var. Italica Plenck) Stems Harvest. Agriculture 12(10), 1519. https://doi.org/10.3390/agriculture12101519

Zhao, Y., Wang, L., Knighton, J., Evaristo, J., Wassen, M., 2021. Contrasting adaptive strategies by *Caragana korshinskii* and *Salix psammophila* in a semiarid revegetated ecosystem. Agric. Forest Meteorol. 300, 108323. https://doi.org/10.1016/j.agrformet.2021.108323

Zhang, P., Pei, C., Liu, Z., Zhang, S., Zhang, Q., Wang, D., 2024. Static mechanical properties testing of Salix and Caragana shrubs based on electrical testing method. J. Inner Mongolia University Technol. Natural Sci. Edition 43(4), 338-342. doi.10.13785/j.cnki.nmggydxxbzrkxb.2024.04.008